Free Radical Biology and Medicine 166 (2021) 178–186

Contents lists available at ScienceDirect

Free Radical Biology and Medicine

journal homepage: www.elsevier.com/locate/freeradbiomed

Original article

Aerobic co-oxidation of hemoglobin and aminoacetone, a putative source of methylglyoxal

Luiz D. Ramos [a,b], Mariana C. Mantovani [a,c,d], Adriano Sartori [e], Fernando Dutra [e], Cassius V. Stevani [a], Etelvino J.H. Bechara [a,c,*]

[a] Departamento de Química Fundamental, Universidade de São Paulo, São Paulo, SP, Brazil
[b] Centro Universitário Anhanguera, UniA, Santo André, SP, Brazil
[c] Instituto de Ciências Ambientais, Químicas e Farmacêuticas, Universidade Federal de São Paulo, Diadema, SP, Brazil
[d] Instituto de Pesquisas Energéticas e Nucleares, Universidade de São Paulo, São Paulo, SP, Brazil
[e] Centro de Ciências Exatas e Tecnologia, Universidade Cruzeiro Do Sul, São Paulo, SP, Brazil

ARTICLE INFO

Keywords:
Aminoacetone
Methylglyoxal
Hemoglobin
α-aminoketones
Electron transfer
Superoxide radical

ABSTRACT

Aminoacetone (1-aminopropan-2-one), a putative minor biological source of methylglyoxal, reacts like other α-aminoketones such as 6-aminolevulinic acid (first heme precursor) and 1,4-diaminobutanone (a microbicide) yielding electrophilic α-oxoaldehydes, ammonium ion and reactive oxygen species by metal- and hemeprotein-catalyzed aerobic oxidation. A plethora of recent reports implicates triose phosphate-generated methylglyoxal in protein crosslinking and DNA addition, leading to age-related disorders, including diabetes. Importantly, methylglyoxal-treated hemoglobin adds four water-exposed arginine residues, which may compromise its physiological role and potentially serve as biomarkers for diabetes. This paper reports on the co-oxidation of aminoacetone and oxyhemoglobin in normally aerated phosphate buffer, leading to structural changes in hemoglobin, which can be attributed to the addition of aminoacetone-produced methylglyoxal to the protein. Hydroxyl radical-promoted chemical damage to hemoglobin may also occur in parallel, which is suggested by EPR-spin trapping studies with 5,5-dimethyl-1-pyrroline-N-oxide and ethanol. Concomitantly, oxyhemoglobin is oxidized to methemoglobin, as indicated by characteristic CD spectral changes in the Soret and visible regions. Overall, these findings may contribute to elucidate the molecular mechanisms underlying human diseases associated with hemoglobin dysfunctions and with aminoacetone in metabolic alterations related to excess glycine and threonine.

1. Introduction

Alpha hydroxy and α-aminoketones are carbohydrate and protein catabolites prone to enolization and further chemical or enzymatic oxidation yielding highly reactive α-oxoaldehyde electrophiles [1–5]. By bearing a vicinal electron-withdrawing carbonyl group, α-oxoaldehydes and aldoses reportedly undergo condensation reactions with the amino groups of basic amino acids such as lysine (Lys) and arginine (Arg) and of nucleobases 2′-deoxyadenosine (dAdo) and 2′-deoxyguanosine (dGuo), yielding Schiff's base. This leads to protein adducts and aggregation and the formation of ethene DNA adducts when accumulated in the tissues of patients suffering from metabolic disorders such as diabetes [6–13].

Methylglyoxal (MG), the simplest and most widely studied α-oxoaldehyde due to its involvement in age-associated diseases, is generated mostly by the spontaneous degradation of the triose phosphates of the glycolytic pathway and subsequent action of methylglyoxal synthase (MS) [14–20]. To a lesser extent, MG is reportedly a product of the cyt P_{450}-catalyzed aerobic oxidation of acetone (a ketone body) and of aminoacetone (AA), a substrate of a semicarbazide-sensitive amine oxidase (SSAO) [14]. Aminoacetone (AA) also is a putative threonine and glycine catabolite produced during reactions catalyzed by the sequential action of L-threonine 3-dehydrogenase (TDH) and 2-amino-3-ketobutyrate CoA ligase (KBL) (Fig. 1) [21]. *In vitro*, aminoacetone has been

Abbreviations: AA, aminoacetone; MG, methylglyoxal; oxyHb, oxyhemoglobin; metHb, methemoglobin; ALA, 5-aminolevulinic acid; DAB, 1,4-diamino-2-butanone.

* Corresponding author. Departamento de Química Fundamental, Instituto de Química, Av. Prof. Lineu Prestes 748, 05508-000, São Paulo, SP, Brazil.
E-mail address: ebechara@iq.usp.br (E.J.H. Bechara).

https://doi.org/10.1016/j.freeradbiomed.2021.02.023
Received 28 December 2020; Received in revised form 10 February 2021; Accepted 13 February 2021
Available online 23 February 2021

shown to undergo non-enzymatic oxidation catalyzed by adventitious iron ions propagated by superoxide ion radicals [17,21–24].

Threonine conversion to aminoacetone is initiated by NAD^+-dependent oxidation to 2-amino-3-ketobutyrate catalyzed by threonine dehydrogenase [22]. Highly unstable, the latter catabolite undergoes spontaneous decarboxylation that yields aminoacetone [27], which is a substrate for a semicarbazide-sensitive amine oxidase, SSAO [3,4,22–24,27], whose products are highly reactive MG and H_2O_2 (Fig. 1). Interestingly, threonine and glycine supplementation of cultures of *Streptomyces sahachiroi,* a soil–dwelling microorganism able to synthesize the antitumor azinomycin A, yields an aminoacetone derivative [21]. Like AA, other α-aminoketones are of biomedical interest, such as 5-aminolevulinic acid (ALA), a heme precursor known to accumulate in blood and other tissues of patients of acquired and inborn porphyria, e.g., in lead poisoning [28–32], intermittent acute porphyria [33,34], and hereditary tyrosinemia Type 1 [35]. In addition, the 1,4-diamino-2-butanone (DAB), a putrescine analogue, acts as a large spectrum microbicide, including against *Trypanosoma cruzi* [36–38].

The α-aminoketones AA, ALA, and DAB have been shown to undergo *in vitro* enolization at physiological pH in phosphate buffer, followed by metal-catalyzed and superoxide-propagated aerobic oxidation to the corresponding α-oxoaldehydes, respectively, MG, 4,5-dioxovaleric acid (DOVA), and 4-amino-2-oxobutanal, plus H_2O_2 and the NH_4^+ ion (Fig. 2) [2,4,37]. Proteins (ferritin, ceruloplasmin, cytochrome *c*), supercoiled plasmid DNA, isolated rat liver mitochondria, insulin-producing cell cultures and rats have been shown, *in vitro* or *in vivo*, to undergo oxidative injury when challenged with α-aminoketones [3,5,39].

Similar to ALA (pK_a 8.1) and DAB (pK_{a1} 7.5; pK_{a2} 9.5), the AA (pK_a 6.8) reaction is believed to be triggered by electron-transfer from tautomeric enol AA [CH_3–C(OH)=$CHNH_2$] to oxygen. This reaction yields a resonant enoyl radical ($AA^{\bullet}$) [CH_3–C($O^{\bullet}$) = $CHNH_2$ ↔ CH_3–CO–$C^{\bullet}NH_2$] and the superoxide radical-anion ($O_2^{\bullet-}$), which propagates the reaction by abstracting one electron from AA (eq. (1)) [5,37,40]. Further electron transfer from $AA^{\bullet}$ to oxygen regenerates $O_2^{\bullet-}$ and forms AA_{imino} (eq. (2)) (CH_3–C(O)–CH=NH), whose hydrolysis yields MG and NH_4^+ ions (eq. (3)). The reaction ends with $O_2^{\bullet-}$ dismutation to H_2O_2 (eq. (4)) and annihilation of $AA^{\bullet}$ by $O_2^{\bullet-}$ radical, which also yields AAimino (eq. (5)).

$$AA + O_2^{\bullet-} + H^+ \rightarrow AA^{\bullet} + H_2O_2 \quad (1)$$

$$AA^{\bullet} + O_2 \rightarrow AA_{imino} + O_2^{\bullet-} + H^+ \quad (2)$$

$$AA_{imino} + H_3O^+ \rightarrow MG + NH_4^+ \quad (3)$$

$$2O_2^{\bullet-} + 2H^+ \rightarrow H_2O_2 + O_2 \quad (4)$$

$$AA^{\bullet} + O_2^{\bullet-} + H^+ \rightarrow AA_{imino} + H_2O_2 \quad (5)$$

Accordingly, AA oxidation to MG is inhibited by the addition of CuZn superoxide dismutase (SOD-1) and its rate of formation increases in response to the addition of the xanthine/xanthine oxidase system, a long-known source of $O_2^{\bullet-}$ radical [1,4]. A remarkable set of potentially toxic reactive species are thus produced by the aerobic oxidation of AA: oxygen- and carbon-centered radicals, H_2O_2, NH_4^+ ion, and electrophilic MG. Hence, AA has been shown to trigger the radical-mediated release of Fe^{2+} ions from ferritin and copper ions in human plasma ceruloplasmin [41–43], inducing Ca^{2+}-mediated membrane permeabilization and oxidative damage to isolated rat liver mitochondria [42] and causing oxidative imbalance and death to insulin-producing RINm5f cells [44]. Moreover, AA has been shown to directly reduce

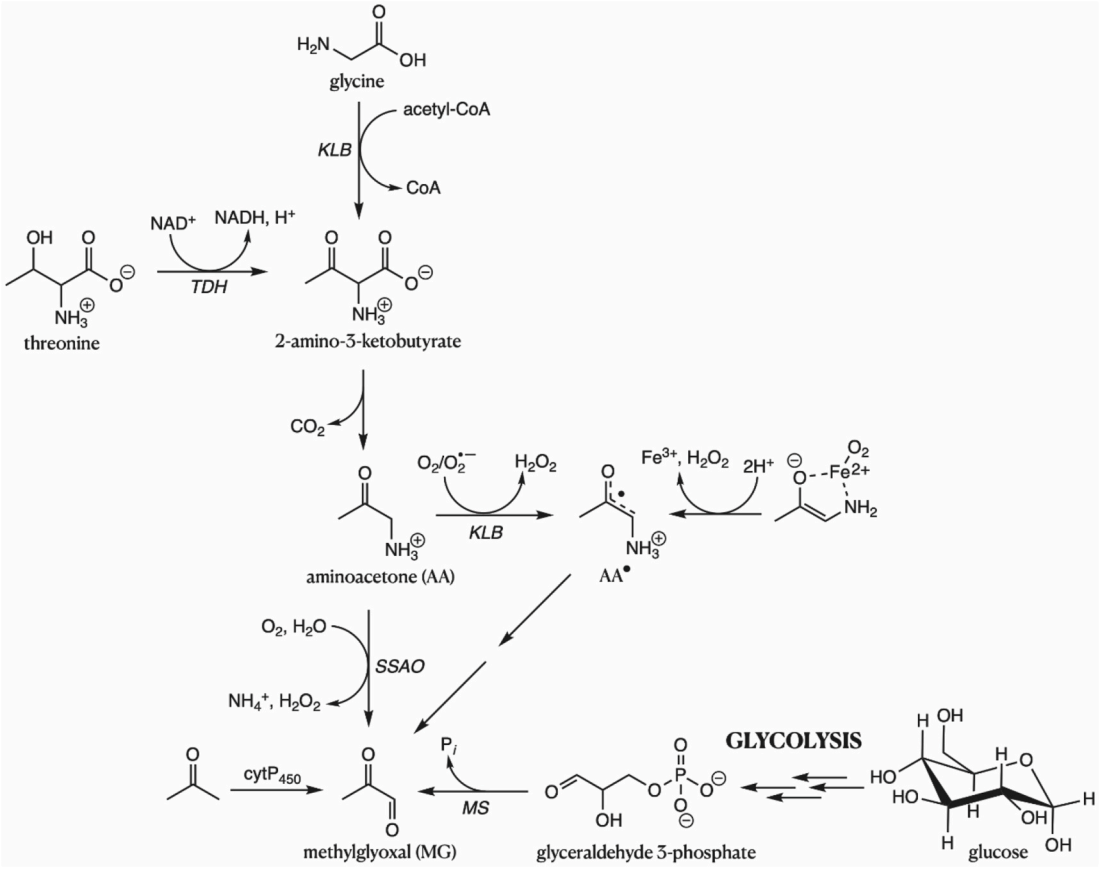

Fig. 1. Proposed pathways for enzymatic generation of methylglyoxal (MG) from triose phosphates [25], acetone [26], and aminoacetone (AA) [4]. Also reported is *in vitro* metal-catalyzed generation of MG from aminoacetone, initiated by a superoxide anion radical source such as the xanthine/xanthine oxidase system [1] or by an H_2O_2-provided oxo-iron AA complex [17].

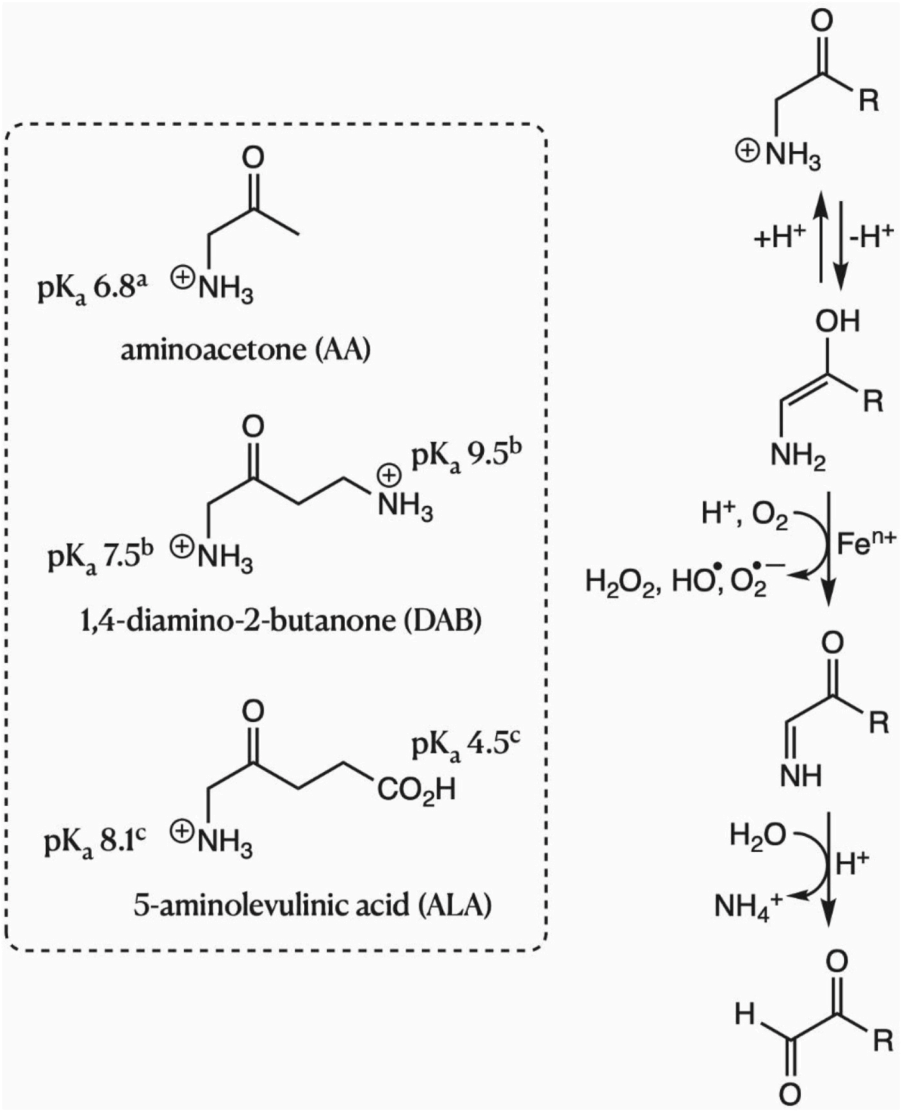

Fig. 2. A-aminoketones reported to undergo metal-catalyzed oxidation by molecular oxygen to the corresponding α-oxoaldehydes and ammonium ion. Values of pKa obtained from Ref. [4][a] [37],[b], and [40][c].

ferricytochrome c to its ferrous form under anaerobiosis, ultimately yielding MG and NH_4^+ ion, and also H_2O_2 when in the presence of oxygen [17]. However, contrary to the studies conducted by Oliveira et al. [45] and more recently by Mercado-Uribe and colleagues [46] on MG-treated cytochrome *c*, no significant alterations in tertiary structure and protein aggregates were found under AA treatment, although enhanced fluorescence intensities were detected, attributable to the oxidation of Trp and Tyr cyt *c* residues [44].

Earlier findings indicate (i) that the physiological concentrations of MG form hydroimidazolone adducts with solvent accessible Arg residues of human hemoglobin (Hb) without heme release [47], and (ii) that bovine oxyhemoglobin (oxyHb) increase the rate of ALA aerobic oxidation to an α-oxoaldehyde (DOVA) chemically similar to MG while being oxidized to methemoglobin (metHb) [2,40]. Consequently, we launched an investigation into oxyHb-induced AA oxidation to MG, under the assumption that it may be relevant to help clarify a possible role of AA in diabetes as a source of MG.

2. Materials and methods

2.1. Reagents

Reagents of the purest quality available and buffer salts were purchased from Sigma-Aldrich (St. Louis, MO). The spin trap 5,5-dimethyl-1-pyrroline-*N*-oxide (DMPO) was obtained from Dojindo Molecular Technologies (Rockville, MD), and HPLC grade solvents were acquired from Merck KGaA (Darmstadt, Germany).

2.2. Synthesis of α-aminoacetone, AA

Alpha-aminoacetone was prepared as described by Hepworth [48], with slight modifications. Briefly, a stoichiometric mixture of glycine, pyridine and acetic anhydride was kept under reflux and stirring for 6 h. Excess reagents were removed by evaporation at reduced pressure without heating, yielding a yellow oil. This oil was dissolved in 6 M HCl and refluxed under Argon atmosphere for 6 h. The solution was concentrated by evaporation at reduced pressure, yielding a brown oil that was recrystallized from ethanol: ether (8:2), sealed in Eppendorf vials in a nitrogen glove box, and stored at −20 °C. Stock solutions of 100 mM AA were prepared in N_2-purged Milli-Q purified water

immediately before use. Elemental analysis of C_3H_8ClNO (Calc./Found): C(32.89/31.92); N(12.79/12.25); H(7.36/7.21). ^{1}HNMR.in D_2O-d2, 200 MHz, δ/ppm): 2.08 (3H, s); 3.88 (2H, s).

2.3. Preparation of oxyHb and metHb

To obtain oxyHb, commercial Hb solution (0.05 mM) was prepared by diluting Hb (Sigma-Aldrich) in Chelex-treated phosphate buffer (50 mM, pH 7.4). Sodium hydrosulfite (SHS) solution was added with SHS: Hb = 1:1 (molar ration), respectively. $NaHSO_3$-treated bovine blood hemoglobin was purified by gel filtration through Sephadex G-25 and quantified spectrophotometrically as already reported [2]. The metHb was prepared in the same way, except that Hb was treated with potassium ferrocyanide.

2.4. Oxygen uptake

A Hansatech oxygraph equipped with a Clark-type electrode was used to measure oxygen uptake by AA (1.0–15 mM) in air-equilibrated buffer at 37 °C, in both the absence and presence of micromolar amounts of oxyHb. Catalase (5 μM) and superoxide dismutase (SOD 1, CuZnSOD) (50 U/mL) were used throughout this work to demonstrate the involvement of H_2O_2 and superoxide species, respectively, in the reaction mechanism.

2.5. UV–vis spectrophotometry

A Varian Cary 50 Bio spectrophotometer was used to record the temporal variations of the absorption spectra of oxyHb (7.8 μM) in the presence and absence of AA (1–5 mM) in 50 mM phosphate buffer at 37 °C. Spectral changes of oxyHb in the range of 300–700 nm were tracked at 2-min intervals for 20 min.

2.6. EPR spin trapping

EPR spin-trapping studies were conducted by using a Bruker EMX spectrometer with the AA/oxyHb reaction mixtures in the presence of 25 mM DMPO and either catalase, SOD or ethanol to verify the intermediacy of oxyradicals. EPR spectra were tracked 3 min after the addition of AA under operating conditions indicated in the figure legends.

2.7. CD analysis

The CD spectra of fivefold diluted 1.0–5.0 mM AA/50 μM oxyHb-containing solutions incubated for 24 h were tracked in the range of 190–450 nm (Far-UV, Near-UV, and Soret regions) at room temperature in a Jasco J-720 spectropolarimeter. Quartz cells with 0.10- and 0.50-cm light paths were used for measurements in the far-UV and near-UV/Soret regions, respectively. All the spectra were corrected by subtracting their backgrounds. The spectra were acquired with 10 nm/min resolution, applying an average of four scans per spectrum. Spectral deconvolution was performed using CONTIN software.

2.8. SDS-PAGE studies

OxyHb (50 μM) was incubated for 2 h at 37 °C with AA (0.0–5.0 mM). The eightfold diluted samples were heated (100 °C for 5 min) in the presence of sample buffer (TRIS pH 6.8 (50 mM); glycerol (10%); SDS (2%); Bromophenol blue (0.1%); 2-Mercaptoethanol (5%). The prepared samples were loaded in 12% polyacrylamide SDS-PAGE gel and separated at 90 V. The protein bands were stained with Coomassie blue dye.

2.9. Statistical analysis

The results obtained from at least three independent experiments were analyzed using one-way ANOVA followed by Dunnett's multiple comparisons test (GraphPad Prism 7), with a significance of $p < 0.05$.

3. Results

3.1. Oxygen uptake studies

As previously reported, 5 mM AA slowly consumes molecular oxygen in air-equilibrated Chelex-treated phosphate buffer (50 mM, pH 7.4 at 37 °C) (Fig. 3d, Table 1), through a reaction propagated by $O_2^{\bullet-}$ radicals and amplified by $HO^\bullet$ radicals formed from superoxide dismutation (eq. (7)) and Fenton-type reaction (eq. (8)). Despite pretreatment with Chelex, residual contaminant transition metal ions must have catalyzed the molecular oxygen-promoted AA oxidation, since autoxidation is spin-forbidden [4,49].

$$Fe^{3+} + O_2^{\bullet-} \rightarrow Fe^{2+} + O_2 \quad (6)$$

$$2O_2^{\bullet-} + 2H^+ \xrightarrow{SOD} H_2O_2 + O_2 \quad (7)$$

$$Fe^{2+} + H_2O_2 \rightarrow Fe^{3+} + HO^\bullet + HO^- \quad (8)$$

Accordingly, oxygen consumption is slowed down by the addition of either SOD (Fig. 3e) or catalase (Fig. 3f), which are known superoxide radical-anion and hydroxyl radical suppressors, respectively. Ten micromolar oxyHb are shown to enhance by fivefold the rate of oxygen uptake (Fig. 3a, Table 1), which is also inhibited in the presence of SOD (Fig. 3b), and much more significantly by that of catalase (Fig. 3c). Initiation of the reaction is here rationalized in terms of previous attachment of AA, an electron donor, to the outer coordination sphere of oxyHb heme Fe(II). This step is based on a similar mechanism long proposed by Wallace and Caughey [50–52] to explain faster oxyHb oxidation to metHb by nucleophiles, and more recently recalled to describe the oxidation of AA catalyzed by cytochrome *c* [17]. Next, concomitant one-electron transfer from coordinated AA and heme Fe(II) to molecular oxygen would yield H_2O_2, a potential source of $HO^\bullet$ radical. Hydroxyl radical could then efficiently initiate the AA superoxide-propagated chain reaction. This hypothesis is consistent with the slower AA oxidation observed in the presence of oxyHb and

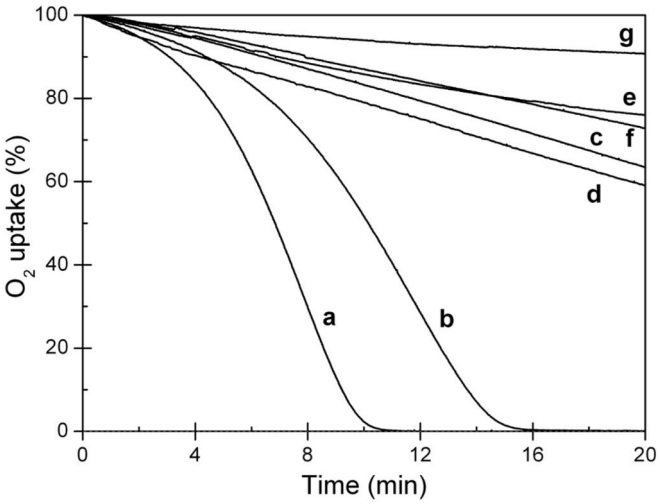

Fig. 3. Effects of SOD and catalase on oxygen consumption by the AA/oxyHb system. The experiments were conducted with 5 mM AA and 10 μM oxyHb in phosphate buffer (50 mM, pH 7.4, 37 °C). AA + oxyHb (**a**); AA + oxyHb + SOD (50 U/mL) (**b**); AA + oxyHb + catalase (5 μM) (**c**); AA (**d**); AA + SOD (50 U/mL) (**e**); AA + catalase (5 μM) (**f**); oxyHb (**g**).

Table 1
Relative rates of O_2 consumption by the AA/oxyHb system in normally aerated 50 mM phosphate buffer, pH 7.4, at 37 °C).

System	O_2 consumption (ΔA/min)[a]
AA + oxyHb (**a**)	5.041 ± 0.009
AA + oxyHb + SOD (**b**)	2.132 ± 0.003
AA + oxyHb + catalase (**c**)	0.553 ± 0.004
AA (**d**)	1.000 ± 0.004
AA + SOD (**e**)	0.443 ± 0.008
AA + catalase (**f**)	0.724 ± 0.005
oxyHb (**g**)	0.465 ± 0.008

[a] Values were normalized for 5,0 mM AA.

catalase (Fig. 3c *vs* d). Similar kinetic effects of the presence of oxyHb, SOD and catalase on the aerobic oxidation of another α-aminoketone, namely ALA, have been reported previously [40]. Ferritin and ceruloplasmin have also previously been shown to amplify AA oxidation through the release of catalytic metal ions [4,41]. In both cases, the intermediacy of reactive $O_2^{\bullet-}$ and H_2O_2 was corroborated by the use of SOD and catalase.

3.2. UV–visible spectrometric analysis

Previous studies have shown that superoxide radical-anion and H_2O_2, produced in the adventitious metal-catalyzed oxidation of ALA and amplified in response to the addition of Fe(III), drive the co-oxidation of oxyHb to metHb [4,40]. Now we report that the addition of AA to oxyHb-containing buffered phosphate solutions also promotes bleaching, hypsochromic shift and heme iron oxidation of oxyHb as a function of AA concentration and incubation time (eq. (9), Fig. 4 and Fig. S1). This is indicated by the decay of oxyHb absorbance at 400, 545, and 577 nm with concomitant increased absorption at 630 nm, and isosbestic points at 350, 523, and 580 nm, which are characteristic of the conversion of oxyHb to metHb [40].

$$AA + oxyHb + O_2 \rightarrow MG + metHb + NH_4^+ + H_2O_2 \quad (9)$$

Spin-trapping EPR experiments with DMPO and ethanol were carried out to confirm the participation of superoxide radical-anion, H_2O_2, and hydroxyl radical intermediates, which were checked by adding

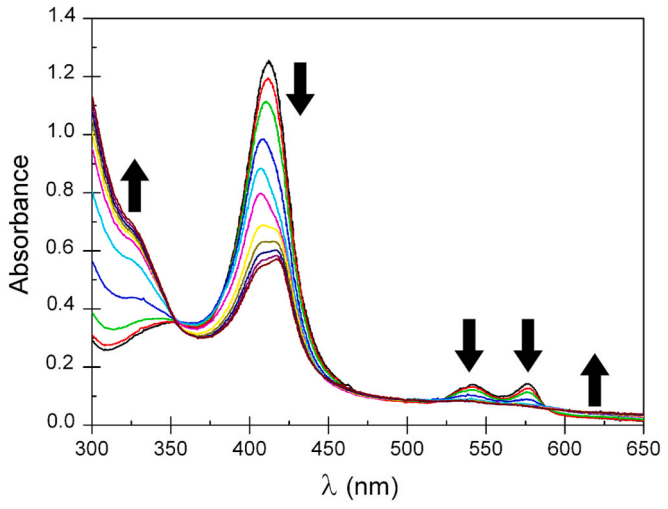

Fig. 4. Spectrophotometric profile of AA and oxyHb co-oxidation. Temporal variations of 7.8 μM hemoglobin spectrum in the presence of 5.0 mM AA in 50 mM phosphate buffer, pH 7.4, at 37 °C, at 2-min intervals for 20 min. 0 min. (**black**); 2 min (**red**); 4 min (**green**); 6 min (blue); 8 min (**cyan**); 10 min (**magenta**); 12 min (**yellow**); 14 min (**dark yellow**); 16 min (**navy**); 18 min (**purple**); 20 min (**wine**). (For interpretation of the references to colour in this figure legend, the reader is referred to the Web version of this article.)

superoxide dismutase and catalase to the AA/oxyHb-containing reaction mixture. The EPR spectra depicted in Fig. 5a–c (black lines) can be assigned to the DMPO-OH spin adduct (4 lines 1:2:2:1; $a_H = a_N = 1.49$ mT) [17,40], whereas the red lines describe a DMPO-α-hydroxyethyl radical [$^{\bullet}CH(OH)–CH_3$] adduct (6 lines; $a_H\beta = 2.28$ mT; $a_N = 1.58$ mT) in the presence of ethanol [53]. The EPR studies with the AA/oxyHb system and the control runs with only AA [40] are depicted in Fig. S2. A 3-min incubation time was adopted to obtain additional information confirming the involvement of the reactive oxygen species in the initiation step (Fig. 5), albeit reflecting an apparent absence of oxyHb effect on the intensity of the EPR spectrum compared to that of the complete system.

As expected, the effect of catalase inhibition observed here (Fig. 5-black-c) clearly predominates over that of SOD (Fig. 5-black-b), which is consistent with the assumption that the reaction is initiated by concomitant two-electron transfer from AA and oxyHb(FeII) to molecular oxygen, yielding H_2O_2 and metHb [2,40]. These findings corroborate the results of the oxymetric studies depicted in Fig. 3, which shows that SOD and catalase decrease the rate of oxygen consumption by the reaction.

EPR spin-trapping experiments in the presence of ethanol (Fig. 5-red) were performed to demonstrate that the four-line signal [DMPO-OH]$^{\bullet}$ adduct does not result from spontaneous [DMPO-OOH]$^{\bullet}$ decomposition ($t_{1/2} = 27$ s at pH 5.0 and 91 s at pH 9.0) [54]. Ethanol does not react with superoxide radical-anion, but is able to donate a hydrogen atom to HO$^{\bullet}$, yielding a stable adduct with DMPO {[DMPO–CHOH–CH_3]$^{\bullet}$, aHβ = 2.28 mT; aN = 1.58 mT} [53]. A six-line spectrum can be assigned to the DMPO-ethanol radical adduct (Fig. 5-red) and it is thus in accordance with the data presented (Fig. 5-black). The use of SOD and catalase only demonstrated a partial inhibitory effect, suggesting that the [DMPO-OH]$^{\bullet}$ radical adduct derives from the Fenton reaction (Fig. 5-black).

3.3. SDS-PAGE experiments

SDS-PAGE studies were performed using an oxyHb-treated AA solution to determine if the system can cause structural and molecular weight damage to the protein (Fig. 6). Albeit not yet identified, hemoglobin alterations by AA-generated products were observed only in the presence of 5 mM AA, which showed a small, but significant decrease in the gel band densitometry. Indeed, numerous studies have reported oxidative damage to proteins promoted by radicals and reactive aldehydes, including α-oxoaldehydes [55,56]. It was previously reported [47] that upon treatment with MG (10 μM–200 mM), hemoglobin (100 μM) undergoes structural and chemical modifications. According to the authors, hemoglobin undergoes condensation reactions with MG (Schiff base formation) in solvent exposed arginine residues, namely Arg-92 and Arg 141 in the α-chain and Arg-40 and Arg-104 in the β-chain, yielding hydroimidazolone derivatives. Two other buried arginine residues – Arg-31 in the α chain and Arg-30 in the β chain – are not modified. The authors suggested that Hb-MG adducts may be harnessed as possible molecular biomarkers of diabetes and other diseases associated with MG accumulation, similarly to non-enzymatically glycated hemoglobin (HbA1c). Noteworthy is the observation of significant hemoglobin alterations only at a higher AA concentration (5 mM), in experiments using up to 200 mM MG [47].

3.4. Circular dichroism studies

The CD spectra of oxyHb in the far-UV range (190–250 nm), near UV (250–350 nm) and the Soret band (390–450 nm), were obtained in the absence and presence of AA in order to verify any spatial structural protein modifications. In response to AA treatment, the far-UV spectrum presents a slight concentration-dependent decrease in the 200 nm peak (Fig. 7A). Spectral deconvolution showed only minor changes in the percentage of protein secondary structure (α-helix = 98.9%; β - sheet =

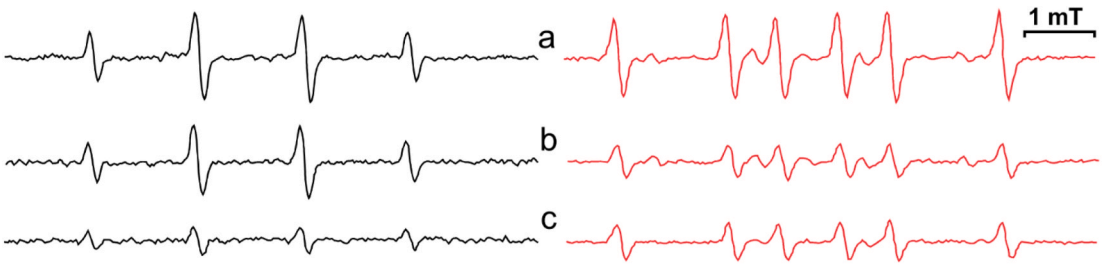

Fig. 5. EPR spin trapping studies of the AA/oxyHb system. Three minutes of incubation of 15 mM AA/150 μM oxyHb using 25 mM DMPO as spin trap in phosphate buffer (50 mM, pH 7.4, at 37 °C) **black lines**, or with 30% ethanol (v/v) **red lines**. AA + oxyHb (**a**); AA + oxyHb + SOD (150 U/mL) (**b**); AA + oxyHb + catalase (5 μM) (**c**). The instrumental conditions were as follows: microwave power = 20 mW, modulation amplitude = 0.1 mT, modulation frequency = 100.00 KHz, time constant = 163.83 ms, receiver gain = 1.1×10^6. (For interpretation of the references to colour in this figure legend, the reader is referred to the Web version of this article.)

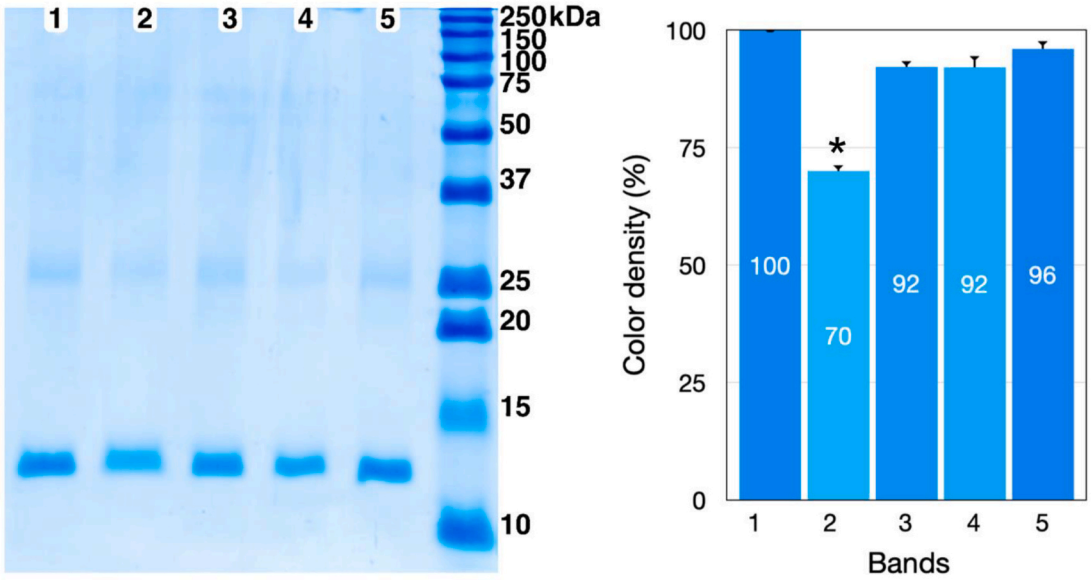

Fig. 6. Hemoglobin band optical densitometries. OxyHb (7.8 μM) were incubated with increasing concentrations of AA and stained with Coomassie blue dye. Fresh Hb control (**1**); Hb + AA (5.0 mM) (**2**), Hb + AA (2.0 mM) (**3**), Hb + AA (1.0 mM) (**4**), incubated Hb control (**5**). Statistical parameters: not significant $p > 0.05$, *$p < 0.05$. (For interpretation of the references to colour in this figure legend, the reader is referred to the Web version of this article.)

1.1%; random structure = 0%). The tertiary structure of the protein (Fig. 7B) proved to be more affected by higher AA concentrations, possibly as a result of the attachment of AA-oxidized MG product to Arg residues of the protein, which would decrease the interaction between aromatics and apoprotein, placing them in a more symmetrical environment [47,57]. The Soret band is also AA-concentration dependent, which may be ascribed to the decreased interaction of the heme moiety with aromatic residues of the protein [58].

4. Discussion

In this report, hemoglobin is shown to undergo co-oxidation with AA to MG via H_2O_2, $O_2^{\bullet-}$, $^{\bullet}OH$ intermediates, with concomitant heme iron oxidation and modification of the secondary and tertiary protein structures. Oxygen uptake measurements show that oxyHb accelerates AA oxidation (fivefold in the experimental conditions of this study; Fig. 3), and is oxidized to metHb (Fig. 4). Unambiguous intermediacy of H_2O_2, and oxyradicals is confirmed by the inhibitory effects of the kinetics of oxygen consumption exerted by the antioxidant enzymes SOD and catalase. Both enzymes inhibit the reaction to some extent, but SOD is more efficient in the absence of oxyHb (Fig. S2), whereas catalase operates mainly in the presence of hemeprotein (Fig. 5) [2,4,5,40,53]. This is in accordance with the proposed mechanisms (equations and Fig. 1). These data are interpreted through different reaction mechanisms of AA metal-catalyzed oxidation or oxyHb-mediated AA oxidation by molecular oxygen, based on previous studies of several metabolites belonging to the classes of α-hydroxycarbonyls, such as dihydroxyacetone phosphate [1], glucose and of α-aminocarbonyls such as ALA [40], AA [4], and DAB [36–38]. In the absence of iron or hemeproteins, these compounds were shown to be oxidized to the corresponding α-oxocarbonyl products via superoxide radical intermediate, which explains the stronger inhibitory effect of added SOD. The lower effect of catalase is due to the greater generation of H_2O_2 from $O_2^{\bullet-}$ dismutation from the Fenton reaction driven by adventitious metals. Once formed, $HO^{\bullet}$ radicals can lead to electron abstraction from AA, thereby amplifying the AA metal-catalyzed oxidation. This is corroborated by the EPR spin trapping studies conducted with DMPO in the absence of oxyHb depicted in Fig. S2-black-a. Conversely, in the presence of oxyHb, the effect of catalase prevails over that of SOD, which has been interpreted as due to previous coordination of AA to the heme iron, followed by *pari passu* one-transfer from both AA and Fe(II) to O_2 yielding H_2O_2, a source of the $HO^{\bullet}$ radical initiator (Fig. 1). The simultaneous operation of the two mechanisms is supported by EPR spin-trapping studies in the presence of ethanol (Fig. 5-red and S2), where both catalase and SOD exhibited a quenching effect, albeit to different degrees, on the DMPO-$^{\bullet}CHOH–CH_3$ adduct signal during the experiment carried out with the AA/oxyHb

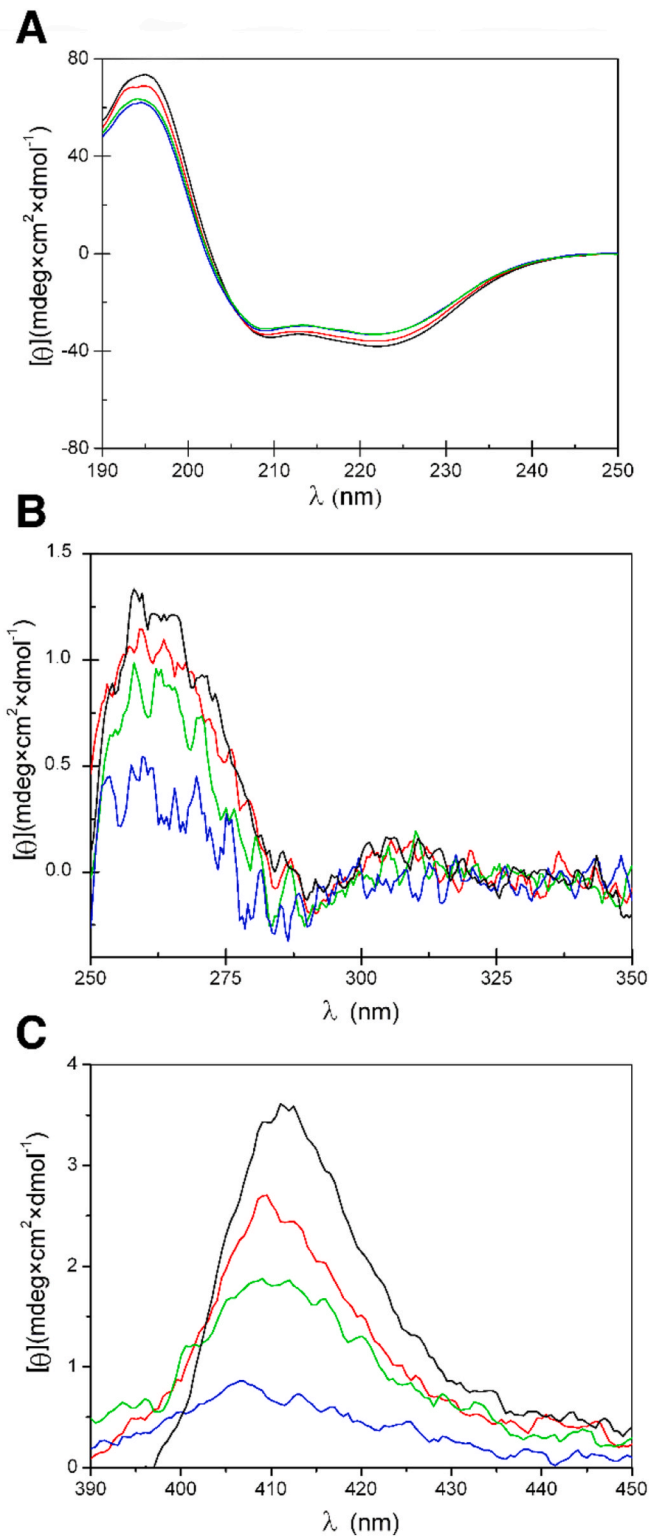

Fig. 7. Effect of AA concentration on the CD spectra of oxyHb in the far-UV (**A**), near UV (**B**), and Soret band region (**C**). Experimental conditions: oxyHb (15 μM) (**black**); oxyHb + AA (1.0 mM) (**red**); oxyHb + AA (2.0 mM) (**green**); oxyHb + AA (5.0 mM) (**blue**). (For interpretation of the references to colour in this figure legend, the reader is referred to the Web version of this article.)

system. The lower efficiency of catalase in the absence of oxyHb (Fig. S2) may also only be apparent because the enzyme-catalyzed decomposition of H_2O_2 partly replenishes the consumed molecular oxygen.

Fragmentation and oligomerization of oxyHb induced by AA were not identified in the SDS-PAGE experiment, as only the native protein monomer band (approximately 14 kDa) was detected. The determination of oxyHb bands by optical densitometry revealed that only a high AA concentration (5 mM) resulted in significantly reducing the intensity of the protein band. This finding is similar to that reported by Wang and Gao in their study of hemoglobin tagging with MG, thus suggesting that SDS-PAGE loss of native oxyHb may be due to the chemical attachment of MG product to water-exposed protein Arg residues [47] and Hb aggregation [55,56].

The UV/visible absorption bands (Fig. 4 and S1) indicate that AA promotes bleaching of the Soret band, causes a hypsochromic shift in the Soret band, and diminishes the absorption intensities attributed to heme iron (545 nm and 577 nm), culminating in the characteristic spectrum of metHb. Additionally, the CD spectra recorded in the UV and visible regions suggest as-yet unidentified secondary and tertiary structural alterations in hemoglobin.

5. Conclusion

In summary, our work presents relevant data that elucidates the role of aminoacetone as a possible contributing source of MG, whose putative accumulation *in vivo* has been implicated in age-related diseases such as diabetes [20] and in threonine disorders such as threoninemia and *cri-du-chat*, a rare inborn disease [4]. Here, we propose that co-oxidation of Hb and aminoacetone occurs by simultaneous one-electron transfer from oxyHb Fe(II) and aminoacetone to molecular oxygen, yielding metHb (FeIII) and H_2O_2, as previously reported by Wallace et al. [51] for electron donors-treated oxyHb and by our group [2,40]. This has now been shown to be accompanied by structural alterations of the apoprotein promoted by AA-generated oxyradicals and electrophilic MG, both species able to elicit adverse effects of AA if accumulated *in vivo* [14].

5.1. Biomedical implications

OxyHb exposure to MG and other α-oxoaldehydes generated by triose phosphates, and to a lesser extent to Thr or Gly/CoA, reportedly leads to structural and oxidative modifications of protein that may impair its biological functions [4,14,39]. Likewise, their determination of HbA1c to evaluate the glycemic status of normal and diabetic individuals led Wang and Gao [47] to suggest that blood indices of Hb-MG adduct may also help clarify pathological conditions linked to excess MG in diabetes, other age-related diseases, and albeit rare, in threoninemia [5]. Moreover, it is important to underscore the biochemical significance of potential oxidative and carbonyl stress triggered by iron- and hemeprotein-catalyzed aerobic oxidation of α-aminocarbonyl metabolites such as ALA, AA and α-amino-substituted aldoses and ketoses for their ability to generate oxy-radicals, H_2O_2, and electrophilic α-dicarbonyls [4,37,40].

Declaration of competing interest

The authors declare that they have no conflict of interests.

Acknowledgements and funding

The authors are grateful to the funding agencies that supported the elaboration of this work. Funding: São Paulo Research Foundation – FAPESP (EJHB 2017/22501–2; LDR 2019/24515–6; CVS 2017/22501–2), by the Brazilian National Council for Scientific and Technological Development – CNPq (EJHB 306460/2016–5), and John Simon Guggenheim Memorial Foundation (EJHB Fellowships). We are indebted to Ohara Augusto and Iseli Nantes for EPR and CD assistance, respectively.

Appendix A. Supplementary data

Supplementary data to this article can be found online at https://doi.org/10.1016/j.freeradbiomed.2021.02.023.

References

[1] T. Mashino, I. Fridovich, Superoxide radical initiates the autoxidation of dihydroxyacetone, Arch. Biochem. Biophys. 254 (2) (1987) 547–551.
[2] H.P. Monteiro, D.S. Abdalla, A. Faljoni-Alàrio, E.J.H. Bechara, Generation of active oxygen species during coupled autoxidation of oxyhemoglobin and delta-aminolevulinic acid, Biochim. Biophys. Acta 881 (1) (1986) 100–106.
[3] Y. Deng, P.H. Yu, Assessment of the deamination of aminoacetone, an endogenous substrate for semicarbazide-sensitive amine oxidase, Anal. Biochem. 270 (1) (1999) 97–102.
[4] F. Dutra, F.S. Knudsen, D. Curi, E.J.H. Bechara, Aerobic oxidation of aminoacetone, a threonine catabolite: iron catalysis and coupled iron release from ferritin, Chem. Res. Toxicol. 14 (9) (2001) 1323–1329.
[5] E.J.H. Bechara, F. Dutra, V.E.S. Cardoso, A. Sartori, K.P.K. Olympio, C.A.A. Penatti, A. Adhikari, N.A. Assunção, The dual face of endogenous α-aminoketones: pro-oxidizing metabolic weapons, Comp. Biochem. Physiol. C Toxicol. Pharmacol. 146 (1) (2007) 88–110.
[6] D.R. Sell, V.M. Monnier, Structure elucidation of a senescence cross-link from human extracellular matrix. Implication of pentoses in the aging process, J. Biol. Chem. 264 (36) (1989) 21597–21602.
[7] T. Douki, J. Onuki, M.H.G. Medeiros, E.J.H. Bechara, J. Cadet, P. Di Mascio, DNA alkylation by 4,5-dioxovaleric acid, the final oxidation product of 5-aminolevulinic Acid, Chem. Res. Toxicol. 11 (2) (1998) 150–157.
[8] A. Vila, K.A. Tallman, A.T. Jacobs, D.C. Liebler, N.A. Porter, L.J. Marnett, Identification of protein targets of 4-hydroxynonenal using click chemistry for ex vivo biotinylation of azido and alkynyl derivatives, Chem. Res. Toxicol. 21 (2) (2008) 432–444.
[9] E.R. Stadtman, R.L. Levine, Free radical-mediated oxidation of free amino acids and amino acid residues in proteins, Amino Acids 25 (3–4) (2003) 207–218.
[10] L.J. Marnett, J.N. Riggins, J.D. West, Endogenous generation of reactive oxidants and electrophiles and their reactions with DNA and protein, J. Clin. Invest. 111 (5) (2003) 583–593.
[11] A.T. Jacobs, L.J. Marnett, Systems analysis of protein modification and cellular responses induced by electrophile stress, Acc. Chem. Res. 43 (5) (2010) 673–683.
[12] I.A. Blair, DNA adducts with lipid peroxidation products, J. Biol. Chem. 283 (23) (2008) 15545–15549.
[13] D. Tamae, P. Lim, G.E. Wuenschell, J. Termini, Mutagenesis and repair induced by the DNA advanced glycation end product n2-1-(carboxyethyl)-2′-deoxyguanosine in human cells, Biochemistry 50 (12) (2011) 2321–2329.
[14] M.P. Kalapos, Methylglyoxal in living organisms: chemistry, biochemistry, toxicology and biological implications, Toxicol. Lett. 110 (3) (1999) 145–175.
[15] N. Murata-Kamiya, H. Kamiya, Methylglyoxal, an endogenous aldehyde, crosslinks DNA polymerase and the substrate DNA, Nucleic Acids Res. 29 (16) (2001) 3433–3438.
[16] P. Matafome, C. Sena, R. Seiça, Methylglyoxal, obesity, and diabetes, Endocrine 43 (3) (2013) 472–484.
[17] A. Sartori, C.M. Mano, M.C. Mantovani, F.H. Dyszy, J. Massari, R. Tokikawa, O. R. Nascimento, I.L. Nantes, E.J.H. Bechara, Ferricytochrome c directly oxidizes aminoacetone to methylglyoxal, a catabolite accumulated in carbonyl stress, PloS One 8 (3) (2013), e57790.
[18] I. Allaman, M. Bélanger, P.J. Magistretti, Methylglyoxal, the dark side of glycolysis, Front. Neurosci. 9 (2015) 23.
[19] L. de Bari, A. Atlante, T. Armeni, M.P. Kalapos, Synthesis and metabolism of methylglyoxal, S-D-lactoylglutathione and D-lactate in cancer and Alzheimer's disease. Exploring the crossroad of eternal youth and premature aging, Ageing Res. Rev. 53 (2019) 100915.
[20] L. Ramachandra Bhat, S. Vedantham, U.M. Krishnan, J.B.B. Rayappan, Methylglyoxal – an emerging biomarker for diabetes mellitus diagnosis and its detection methods, Biosens. Bioelectron. 133 (2019) 107–124.
[21] V. Sharma, G.T. Kelly, J. Foulke-Abel, C.M.H. Watanabe, Aminoacetone as the penultimate precursor to the antitumor agent azinomycin A, Org. Lett. 11 (17) (2009) 4006–4009.
[22] G.A. Lyles, J. Chalmers, The metabolism of aminoacetone to methylglyoxal by semicarbazide-sensitive amine oxidase in human umbilical artery, Biochem. Pharmacol. 43 (7) (1992) 1409–1414.
[23] M. Ravichandran, S. Priebe, G. Grigolon, L. Rozanov, M. Groth, B. Laube, R. Guthke, M. Platzer, K. Zarse, M. Ristow, Impairing L-threonine catabolism promotes healthspan through methylglyoxal-mediated proteohormesis, Cell Metabol. 27 (4) (2018) 914–925, e5.
[24] C. Li, Z. Wang, X. Li, J. Chen, Effects of semicarbazide-sensitive amine oxidase inhibitors on morphology of aorta and kidney in diabetic rats, BMC Endocr. Disord. 19 (1) (2019) 59.
[25] S.A. Phillips, P.J. Thornalley, The formation of methylglyoxal from triose phosphates, Eur. J. Biochem. 212 (1) (1993) 101–105.
[26] M.P. Kalapos, On the mammalian acetone metabolism: from chemistry to clinical implications, Biochim. Biophys. Acta Gen. Subj. 1621 (2) (2003) 122–139.
[27] A. Schmidt, J. Sivaraman, Y. Li, R. Larocque, J.A. Barbosa, C. Smith, A. Matte, J. D. Schrag, M. Cygler, Three-dimensional structure of 2-amino-3-ketobutyrate CoA ligase from Escherichia coli complexed with a PLP-substrate intermediate: inferred reaction mechanism, Biochemistry 40 (17) (2001) 5151–5160.
[28] C.A. Costa, G.C. Trivelato, A.M. Pinto, E.J. Bechara, Correlation between plasma 5-aminolevulinic acid concentrations and indicators of oxidative stress in lead-exposed workers, Clin. Chem. 43 (7) (1997) 1196–1202.
[29] S.N. Kelada, E. Shelton, R.B. Kaufmann, M.J. Khoury, δ-Aminolevulinic acid dehydratase genotype and lead toxicity: a HuGE Review, Am. J. Epidemiol. 154 (1) (2001) 1–13.
[30] H. Needleman, Lead poisoning, Annu. Rev. Med. 55 (1) (2004) 209–222.
[31] S. Sassa, Modern diagnosis and management of the porphyrias, Br. J. Haematol. 135 (3) (2006) 281–292.
[32] K.P. Olympio, C.G. Gonçalves, F.J. Salles, A.P. Ferreira, A.S. Soares, M.A. Buzalaf, M.R. Cardoso, E.J. Bechara, What are the blood lead levels of children living in Latin America and the Caribbean? Environ. Int. 101 (2017) 46–58.
[33] B. Wang, S. Rudnick, B. Cengia, H.L. Bonkovsky, Acute hepatic porphyrias: review and recent progress, Hepatol. Commun. 3 (2) (2019) 193–206.
[34] A. Adhikari, C.A.A. Penatti, R.R. Resende, H. Ulrich, L.R.G. Britto, E.J.H. Bechara, 5-Aminolevulinate and 4, 5-dioxovalerate ions decrease GABAA receptor density in neuronal cells, synaptosomes and rat brain, Brain Res. 1093 (1) (2006) 95–104.
[35] M.E. Rocha, B. Bandy, C.A. Costa, M.P. de Barros, A.M. Pinto, E.J. Bechara, Iron mobilization by succinylacetone methyl ester in rats. A model study for hereditary tyrosinemia and porphyrias characterized by 5-aminolevulinic acid overload, Free Radic. Res. 32 (4) (2000) 343–353.
[36] C.O. Soares, W. Colli, E.J.H. Bechara, M.J.M. Alves, 1,4-Diamino-2-butanone, a putrescine analogue, promotes redox imbalance in Trypanosoma cruzi and mammalian cells, Arch. Biochem. Biophys. 528 (2) (2012) 103–110.
[37] C.O. Soares, M.J.M. Alves, E.J.H. Bechara, 1,4-Diamino-2-butanone, a wide-spectrum microbicide, yields reactive species by metal-catalyzed oxidation, Free Radic. Biol. Med. 50 (12) (2011) 1760–1770.
[38] C.O. Soares, M. Boiani, L.J. Marnett, E.J. Bechara, Cytotoxicity of 1,4-diamino-2-butanone, a putrescine analogue, to RKO cells: mechanism and redox imbalance, Free Radic. Res. 47 (9) (2013) 672–682.
[39] Y. Hiraku, J. Sugimoto, T. Yamaguchi, S. Kawanishi, Oxidative DNA damage induced by aminoacetone, an amino acid metabolite, Arch. Biochem. Biophys. 365 (1) (1999) 62–70.
[40] H.P. Monteiro, D.S.P. Abdalla, O. Augusto, E.J.H. Bechara, Free radical generation during δ-Aminolevulinic acid autoxidation: induction by hemoglobin and connections with porphyrinpathies, Arch. Biochem. Biophys. 271 (1) (1989) 206–216.
[41] F. Dutra, M.R. Ciriolo, L. Calabrese, E.J.H. Bechara, Aminoacetone induces oxidative modification to human plasma ceruloplasmin, Chem. Res. Toxicol. 18 (4) (2005) 755–760.
[42] F. Dutra, E.J.H. Bechara, Aminoacetone induces iron-mediated oxidative damage to isolated rat liver mitochondria, Arch. Biochem. Biophys. 430 (2) (2004) 284–289.
[43] F. Dutra, D. Araki, E.J.H. Bechara, Aminoacetone induces loss of ferritin ferroxidase and iron uptake activities, Free Radic. Res. 37 (10) (2003) 1113–1121.
[44] A. Sartori, H.M. Garay-Malpartida, M.F. Forni, R.I. Schumacher, F. Dutra, M. C. Sogayar, E.J.H. Bechara, Aminoacetone, a putative endogenous source of methylglyoxal, causes oxidative stress and death to insulin-producing RINm5f cells, Chem. Res. Toxicol. 21 (9) (2008) 1841–1850.
[45] L.M. Oliveira, R.A. Gomes, D. Yang, S.R. Dennison, C. Família, A. Lages, A. V. Coelho, R.M. Murphy, D.A. Phoenix, A. Quintas, Insights into the molecular mechanism of protein native-like aggregation upon glycation, Biochim. Biophys. Acta 1834 (6) (2013) 1010–1022.
[46] H. Mercado-Uribe, M. Andrade-Medina, J.H. Espinoza-Rodríguez, M. Carrillo-Tripp, C.Q. Scheckhuber, Analyzing structural alterations of mitochondrial intermembrane space superoxide scavengers cytochrome-c and SOD1 after methylglyoxal treatment, PloS One 15 (4) (2020), e0232408.
[47] Y. Gao, Y. Wang, Site-selective modifications of arginine residues in human hemoglobin induced by methylglyoxal, Biochemistry 45 (51) (2006) 15654–15660.
[48] J.D. Hepworth, Aminoacetone semicarbazone hydrochloride, Org. Synth. 45 (1973) 27–29.
[49] D.M. Miller, G.R. Buettner, S.D. Aust, Transition metals as catalysts of "autoxidation" reactions, Free Radic. Biol. Med. 8 (1) (1990) 95–108.
[50] W.J. Wallace, R.A. Houtchens, J.C. Maxwell, W.S. Caughey, Mechanism of autooxidation for hemoglobins and myoglobins. Promotion of superoxide production by protons and anions, J. Biol. Chem. 257 (9) (1982) 4966–4977.
[51] W.J. Wallace, W.S. Caughey, Mechanism for the autoxidation of hemoglobin by phenols, nitrite and "oxidant" drugs. Peroxide formation by one electron donation to bound dioxygen, Biochem. Biophys. Res. Commun. 62 (3) (1975) 561–567.
[52] W.S. Caughey, C.H. Barlow, J.C. Maxwell, J.A. Volpe, W.J. Wallace, Reactions of oxygen with hemoglobin, cytochrome c oxidase and other hemeproteins, Ann. N. Y. Acad. Sci. 244 (1) (1975) 1–9.
[53] E. Finkelstein, G.M. Rosen, E.J. Rauckman, Spin trapping. Kinetics of the reaction of superoxide and hydroxyl radicals with nitrones, J. Am. Chem. Soc. 102 (15) (1980) 4994–4999.
[54] B.E. Britigan, T.L. Roeder, G.R. Buettner, Spin traps inhibit formation of hydrogen peroxide via the dismutation of superoxide: implications for spin trapping the hydroxyl free radical, Biochim. Biophys. Acta Gen. Subj. 1075 (3) (1991) 213–222.
[55] A. Iram, T. Alam, J.M. Khan, T.A. Khan, R.H. Khan, A. Naeem, Molten globule of hemoglobin proceeds into aggregates and advanced glycated end products, PloS One 8 (8) (2013), e72075.
[56] L.J. Deterding, D.C. Ramirez, J.R. Dubin, R.P. Mason, K.B. Tomer, Identification of free radicals on hemoglobin from its self-peroxidation using mass spectrometry and

immuno-spin trapping: observation of a histidinyl radical, J. Biol. Chem. 279 (12) (2004) 11600–11607.
[57] D.A. Dolgikh, R.I. Gilmanshin, E.V. Brazhnikov, V.E. Bychkova, G.V. Semisotnov, S.Y. Venyaminov, O.B. Ptitsyn, α-Lactalbumin: compact state with fluctuating tertiary structure? FEBS Lett. 136 (2) (1981) 311–315.
[58] M. Nagai, Y. Nagai, K. Imai, S. Neya, Circular dichroism of hemoglobin and myoglobin, Chirality 26 (9) (2014) 438–442.